Structural Variation in Transition-Metal Bispidine Compounds

Peter Comba,* Marion Kerscher, Michael Merz, Vera Müller, Hans Pritzkow, Rainer Remenyi, Wolfgang Schiek, and Yun Xiong[a]

Dedicated to Professor Gottfried Huttner on the occasion of his 65th birthday

Abstract: The experimentally determined molecular structures of 40 transition metal complexes with the tetradentate bispyridine-substituted bispidone ligand, 2,4-bis(2-pyridine)-3,7-diazabicyclo[3.3.1]nonane-9-one $[M(bisp)XYZ]^{n+}$; M = Cr^{III}, Mn^{II}, Fe^{II}, Co^{II}, Cu^{II}, Cu^{I}, Zn^{II}; X, Y, Z = mono- or bidentate co-ligands; penta-, hexa- or heptacoordinate complexes) are characterized in detail, supported by force-field and DFT calculations. While the bispidine ligand is very rigid (N3 $\cdots$ N7 distance = 2.933 ± 0.025 Å), it tolerates a large range of metal–donor bond lengths (2.07 Å $< \Sigma(M{-}N)/4 < 2.35$ Å). Of particular interest is the ratio of the bond lengths between the metal center and the two tertiary amine donors (0.84 Å $< M{-}N3/M{-}N7 < 1.05$ Å) and the fact that, in terms of this ratio there seem to be two clusters with M−N3 < M−N7 and M−N3 ≥ M−N7. Calculations indicate that the two structural types are close to degenerate, and the structural form therefore depends on the metal ion, the number and type of co-ligands, as well as structural variations of the bispidine ligand backbone. Tuning of the structures is of importance since the structurally differing complexes have very different stabilities and reactivities.

Keywords: bond-stretch isomerism · complementarity · elasticity · N ligands · structure correlation · transition metals

Introduction

The most common type of bonding isomerism in transition metal coordination compounds results from ambidentate ligands, such as NCS^-, NO_2^-, and CN^-; less frequently discussed examples include substituted tetrazolates and biologically important substrates, such as urea, purines, and pyrimidines.[1] Other types of structural variation are the various bonding modes of dioxygen in hemocyanin and corresponding model compounds;[2–7] metal–metal bonding isomerism as in face-shared bis(octahedral) dimetal-nonachloro complexes[8–10] and translational isomers in coordination compounds and supramolecular systems.[11–16] The various bonding modes may be enforced by the co-ligands (for example, in hemocyanin model compounds, that is, these are then only isomers with respect to the metal-O_2 core), by the environment (crystal lattice, for example, in the bis(octahedral) dimetal compounds; or solvent and temperature, for example, with some hemocyanin models) or by changing oxidation states and/or pH (e.g., in translational isomerism; again, these are then not true isomers). Applications of these various types of structural variations ("isomerism") include the tuning of specific properties, such as catalytic activities and the development of switches and sensors.

A vigorous controversy evolved around early theoretical and experimental reports of bond-stretch or distortional isomerism.[17–24] Bond-stretch isomers are molecules which differ only in the length of one or several bonds. Spin-crossover compounds (and metal–metal bonding isomerism, as described above, as well as the various bonding modes of dioxygen) might be classified as distortional isomers; however, on a more rigorous basis, bond-stretch isomers are defined as species on a single potential energy surface with two (or more) minima.[25, 26] Even with this restrictive definition, a clear distinction is not always obvious, as was recently shown on the basis of experimental and theoretical studies with a dichloro-bridged diruthenium complex.[27–29] Experimental studies as well as a thorough theoretical analysis revealed that the early examples of distortional isomerism were caused by artifacts.[23, 30–33] While examples of "true" bond-stretch isomerism are still rare[34–37] there have been recent examples of interesting structural and spectroscopic studies in this field, although (partly for good reason) not all of them have been discussed as distortional iso-

[a] Prof. Dr. P. Comba, M. Kerscher, Dr. M. Merz, V. Müller, Dr. H. Pritzkow, Dr. R. Remenyi, Dr. W. Schiek, Y. Xiong
Anorganisch-Chemisches Institut
Universität Heidelberg
Im Neuenheimer Feld 270, 69120 Heidelberg (Germany)
Fax: (+49) 6221-546617
E-mail: comba@akcomba.oci.uni-heidelberg.de

Supporting information for this article (Plot of M−N3/M−N7 versus ν) is available on the WWW under http://www.chemeurj.org or from the author.

  0947-6539/02/0824-5750 $ 20.00+.50/0

mers.[38, 39] In blue copper proteins, another relevant example, quantum mechanical calculations predict that there are two nearly degenerate ground states with significantly different geometries,[40–43] and the recently published observation of a temperature-dependent, reversible color change of a cupredoxine mutant[44] can also be interpreted on this basis and might therefore be a genuine case of distortional isomerism.[45]

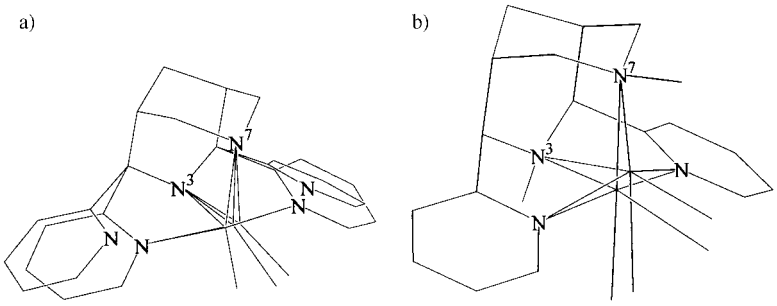

Scheme 2.

Tetradentate bispidine-type ligands with two tertiary amine and two pyridine donors (Scheme 1) have a very rigid sparteine-type backbone and are known to enforce, for

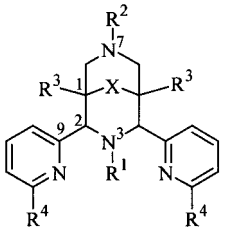

Scheme 1. L^{1a}: R^1, $R^2 = CH_3$; $R^3 = COOCH_3$; $R^4 = H$; X = C=O. L^{1b}: R^1, $R^2 = CH_3$; $R^3 = COOCH_3$; $R^4 = H$; $X = C(OH)_2$. L^{1c}: R^1, $R^2 = CH_3$; $R^3 = COOCH_3$; $R^4 = H$; X = C(OH)(OCH$_3$). L^{1d}: R^1, $R^2 = CH_3$; $R^3 = COOCH_3$; $R^4 = H$; X = CHOH. L^2: $R^1 = CH_3$, $R^2 = (CH_2)_2OH$, $R^4 = H$; (R^3, X, a–d: as for L^1). L^3: R^1, $R^2 = CH_3$; $R^4 = CH_3$ (R^3, X, a–d: as for L^1). L^4: $R^1 = CH_3$, $R^2 = (CH_2)_2L$; $R^4 = H$; (R^3, X, a–d: as for L^1). L^5: $R^1 = CH_3$, $R^2 = (CH_2)_3L$; $R^4 = H$; (R^3, X, a–d: as for L^1).

pentacoordinate metal centers, a square-pyramidal coordination polyhedron with one free in-plane coordination site.[46, 47] This unusual and rigid coordination geometry is of interest for the stabilization and activation of substrates and has been the reason for an increasing interest in bispidine coordination chemistry. Four-coordinate (distorted tetrahedral coordination, tridentate bispidine, one monodentate co-ligand, copper(I)),[48, 49] five-coordinate (square-pyramidal coordination, one monodentate co-ligand, copper(I), copper(II), zinc(II)),[6, 48–51] six-coordinate (octahedral coordination, one bidentate or two monodentate co-ligands, chromium(III), manganese(II), iron(II), cobalt(II), copper(II))[49, 50–53] and seven-coordinate (pentagonal-bipyramidal coordination, one mono- and one bidentate co-ligand, manganese(II)) complexes have been observed and structurally analyzed. Note, that in this publication we concentrate on tetradentate bispidine ligands of the type shown in Scheme 1; bispidine-type ligands with other donor sets, penta- and hexadentate, as well as macrocyclic ligands[50, 53–57] will not be discussed here in detail.

Three types of isomerism with bispidine coordination compounds have been discovered: 1) an equilibrium between four- and five-coordinate structures (tri- and tetradentate bispidine, true constitutional isomerism; Scheme 2a).[48] 2) Four bonding modes of tetrachlorocatecholate to copper(II)– or biscopper(II)–bispidine complexes, that is, monodentate, two different chelating modes (equatorial-equatorial, that is, the usual mode for copper(II) catecholate complexes, and equatorial–axial); and bridging between two bispidine-copper(II) sites, true isomerism in some cases.[51] 3) A dislocation of the metal ion in the cavity, leading to geometries with varying ratios of M–N3/M–N7 bond lengths (see Scheme 2b, distortional isomerism with respect to the metal-bispidine fragment if these are structures with the same metal center and if the varying ratios correspond to discrete minima). Based on the available structural information (40 relevant crystal structure datasets), approximate density functional theory (DFT) and empirical force-field calculations (MM) this latter structural variation is analyzed here in detail. An answer to the question as to whether there is a continuum or two (or more) separate clusters of structures and the ability to tune the structures, are not only of importance in terms of the question of distortional isomerism (note again that isomerism in this context is only an appropriate term with respect to the M(bispidine) fragment and if compounds with the same metal center and bispidine ligand are discussed) but also for the variation of the reactivity (catalytic activity) and stability of bispidine coordination compounds. Recent studies have shown that copper(II) compounds with a long Cu–N7 axis lead to unusually stable peroxodicopper(II) complexes, while the others do not.[6, 49] There are large differences in reduction potential, electron-transfer rate, and bond strength to the co-ligands between the two forms.[49, 50, 58] Copper(II) complexes with a long Cu–N3 bond are at least twice as efficient as catalysts for the aziridination of styrene than the others.[50] Also, the two structural forms of iron(II) complexes with pentadentate bispidine derivatives (one additional pyridine donor) lead, upon oxidation with H_2O_2, to low-spin iron(III) hydroperoxo complexes with significantly different stabilities and oxidation catalytic reactivities.[59]

Results and Discussion

Forty datasets of experimentally determined structures of transition-metal compounds with tetradentate bispidine ligands with an N_2py_2 donor set (Scheme 1) and one (tetragonal pyramidal), two (pseudo-octahedral), or three additional donors (pentagonal bipyramidal) are known so far. These include complexes with chromium(III), manganese(II),[60] iron(II),[53] cobalt(II),[52] copper(I),[48, 49] copper(II)[6, 48–51] and zinc(II). ORTEP[61] plots of the structures not published elsewhere are given in Figure 1. This also includes two structures with seven-

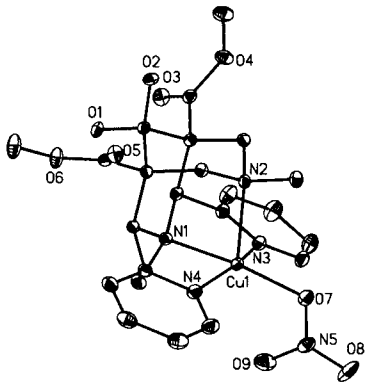

10

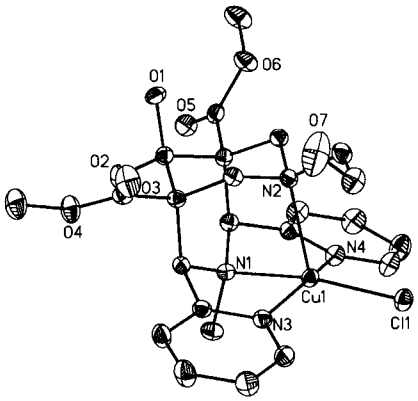

11

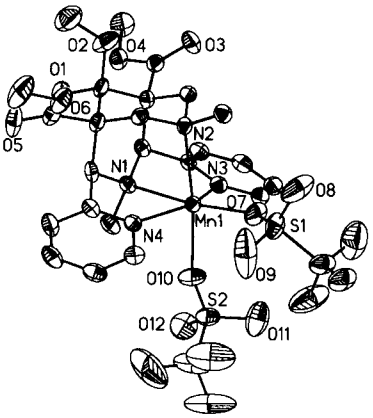

21

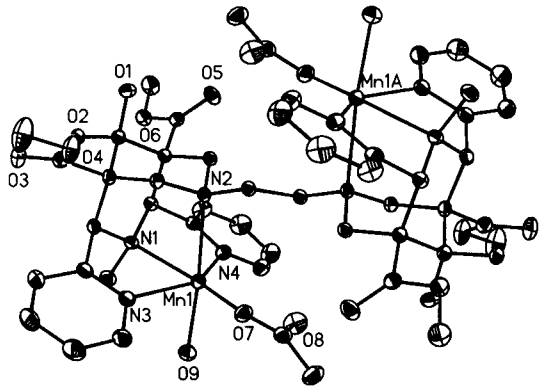

22

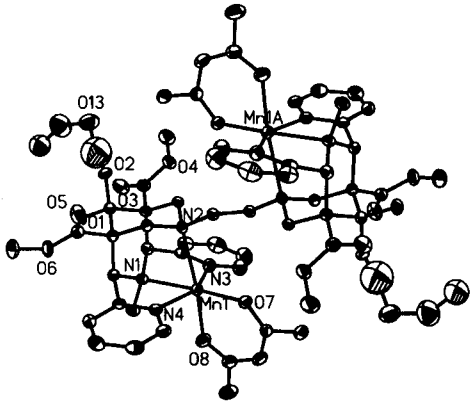

23

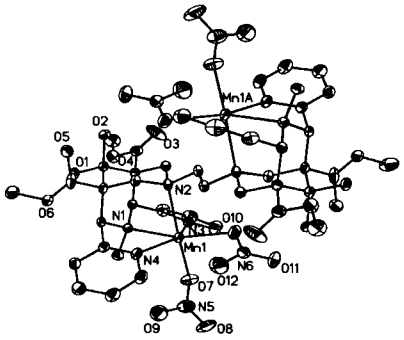

24

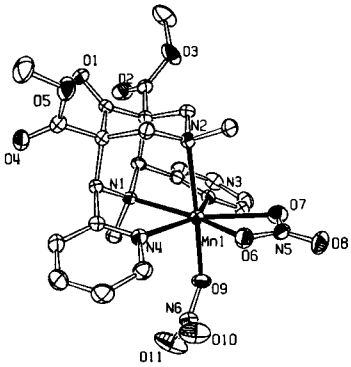

25

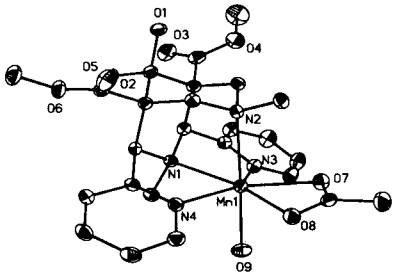

26

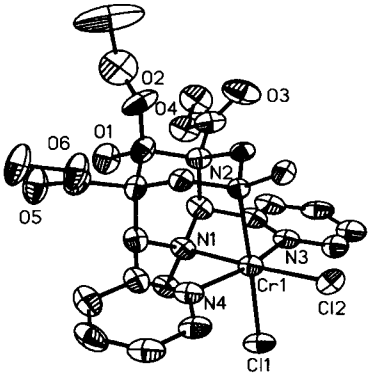

27

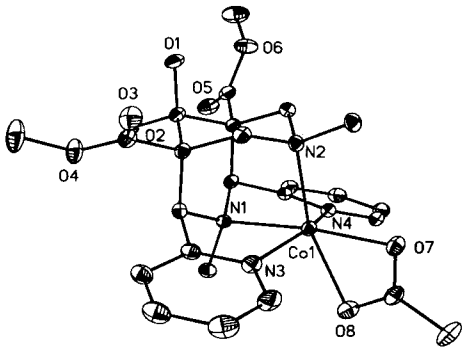

29

0947-6539/02/0824-5752 $ 20.00+.50/0 *Chem. Eur. J.* **2002**, *8*, No. 24

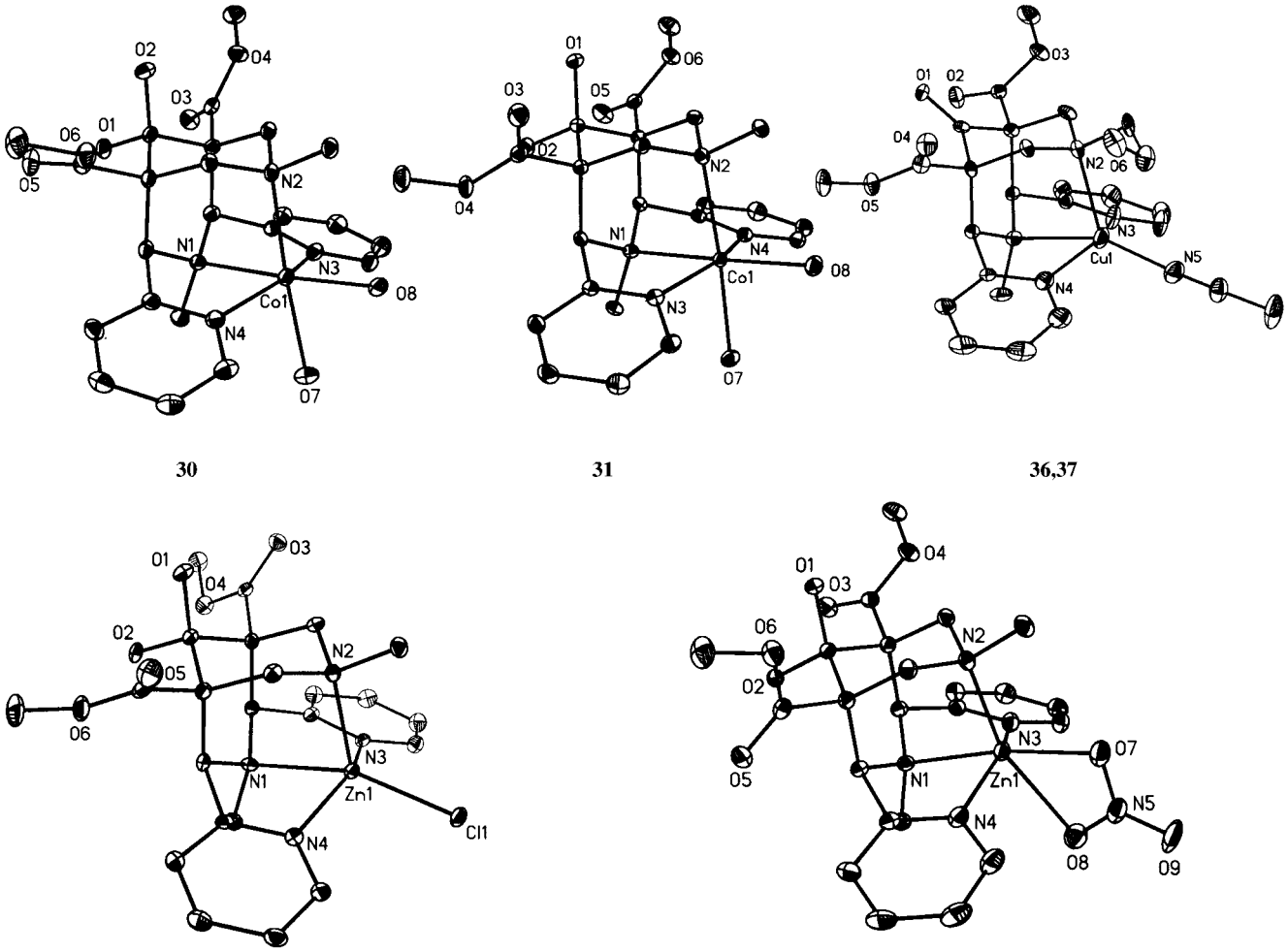

30 **31** **36,37**

38,39 **40**

Figure 1. ORTEP[61] plots of the molecular cations (distances in Å) of **10** (Cu–O7 1.98, Cu–O9 2.61), **11** (Cu–Cl 2.22), **21** (Mn–O7 2.11, Mn–O10 2.16), **22** (Mn–O7 2.13, Mn–O9 2.15), **23** (Mn–O7 2.06, Mn–O8 2.12), **24** (Mn–O10 2.22, Mn–O12 2.57, Mn–O7 2.18), **25** (Mn–O6 2.28, Mn–O7 2.41, Mn–O9 2.17), **26** (Mn–O8 2.43, Mn–O7 2.26, Mn–O9 2.19), **27** (Cr–Cl2 2.29, Cr–Cl1 2.31), **29** (Co–O7 2.06, Co–O8 2.23) **30** (Co–O8 2.04, Co–O7 2.20), **31** (Co–O8 2.07, Co–O7 2.14), **36**, **37** (Cu–N5 1.91), **38**, **39** (Zn–Cl 2.26), **40** (Zn–O7 2.09, Zn–O8 2.37).

coordinate (pentagonal bipyramidal) manganese(II) centers. Although many manganese(II) coordination compounds are six-coordinate, seven-coordination is not uncommon with large metal centers, such as manganese(II), ligands with a rather small and inflexible bite, such as bispidines, and metal centers with little electronic demand, such as high-spin d^5 systems.

The rigidity of the bispidine backbone is demonstrated in Figure 2. These are plots from crystal structures and corresponding overlay plots (excluded in the overlay plots are the structure of the metal-free ligand (see Figure 2b) and structures involving the methylated ligand (L^3); co-ligands and substituents to the ligand backbone are omitted). In Figure 2a, the metal centers and co-ligands have been deleted from the structures. Figure 2b shows the structure of the metal-free ligand (rotation of the pyridine groups around the C^2–C^9 bonds (see Scheme 1 for the numbering scheme) by $\approx 180^\circ$ with respect to the coordinated ligand).[48] This indicates that the ligand is complementary for square-pyramidal and cis-octahedral coordination geometries.[47, 62, 63] Figure 2c is the averaged ligand structure from Figure 2a with all 40 metal centers included; Figure 2d, e show two views of a plot similar to that of Figure 2c but with only three metal ion positions included, namely, those of copper(II), copper(I), and manganese(II) (see **1**, **32**, **19** in Table 1; an arbitrary choice but typical for the three clusters, see below, and also Scheme 2b). This is a visualization of the dislocation of the metal center within the rigid bispidine cavity; distances between the three metal centers in Figure 2d, e are up to ≈ 0.5 Å.

Selected geometric parameters of the experimental structures discussed here are given in Table 1. Not included in the structural analysis are the co-ligands, that is, we only characterize the M–bispidine fragments (distances to the co-ligands are given in the caption of Figure 1). The rigidity of the bispidine backbone is further highlighted by a constant N3$\cdots$N7 distance (2.933 ± 0.025 Å) but a large variation of the metal ion size ($2.07\ \text{Å} < \Sigma(\text{M–N})/4 < 2.35\ \text{Å}$) and the M–N3/M–N7 ratio ($0.84\ \text{Å} < \text{M–N3/M–N7} < 1.05\ \text{Å}$). A significant variation is also apparent for the torsion of the pyridine substituents ($28^\circ < \varnothing(C^2\text{–}C^9) < 45^\circ$; this is also

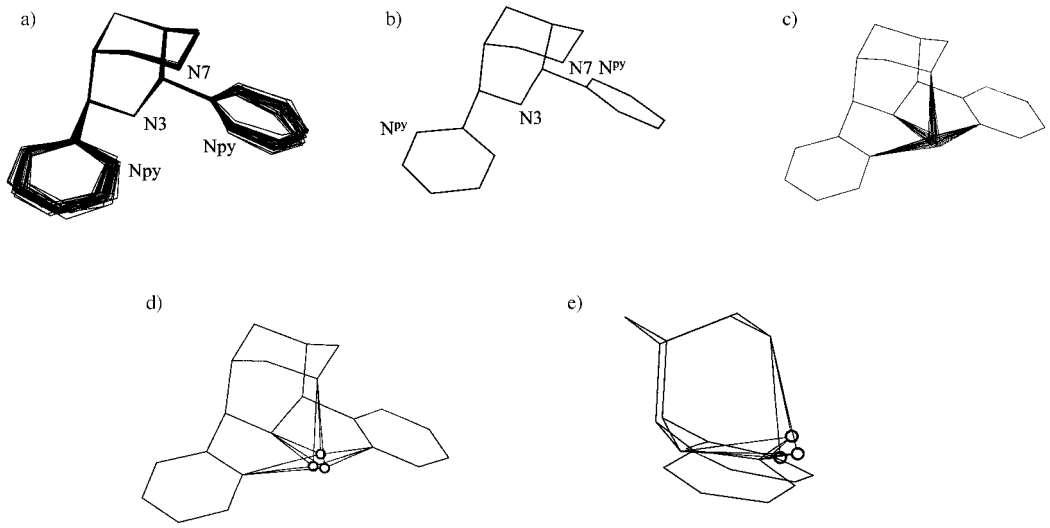

Figure 2. Plots of the bispidine ligand backbone and the metal ion position, based on experimentally determined coordinates, of the structures from Table 1 and that of the metal-free ligand.[48] a) Overlay of the ligand backbone of the 40 structures from Table 1, two structures of L^3 excluded. b) Metal-free ligand. c) Average structure from (a) and overlay of all metal centers. d, e) Average structure from (a) and overlay of the metal centers from structures **1**, **19**, **32** from Table 1.

Table 1. Structural parameters of forty $[M(bispidine)X_n]^{m+}$ complexes

	Metal ion	Ligand	Co-ligands[a]	CN	Ref.	M–N3	M–N7	M–py1	M–py2	Σ(M–N)	M–N3/ M–N7	M–N^{am}/ M–N^{py}	N3···N7	py1···py2	$\varnothing_{av}$ (C2–C9)	τ	h	v
1	Cu(II)	L^{1b}	Cl	5	[6]	2.04	2.27	2.02	2.02	8.35	0.9	1.07	2.92	3.97	35	30	1.58	−0.17
2	Cu(II)	L^{4b}	$NCCH_3$	5	[50]	2.01	2.34	1.99	2.01	8.35	0.86	1.09	2.93	3.94	34	30	1.60	−0.24
3	Cu(II)	L^{5b}	Cl	5	[50]	2.03	2.36	2.01	2.03	8.43	0.86	1.09	2.91	3.94	33	30	1.63	−0.25
4	Cu(II)	L^{5b}	Cl	5	[50]	2.03	2.30	1.99	2.02	8.34	0.88	1.08	2.92	3.97	31	15	1.59	−0.20
5	Cu(II)	L^{1b}	cat	6	[51]	2.04	2.43	2.01	2.03	8.51	0.84	1.11	2.92	3.99	34	25	1.68	−0.30
6	Cu(II)	L^{1b}	Hcat	5	[51]	2.03	2.31	1.98	1.99	8.31	0.88	1.09	2.92	3.91	33	25	1.60	−0.21
7	Cu(II)	L^{1b}	Hcat	5	[51]	2.02	2.32	1.99	1.99	8.32	0.87	1.09	2.91	3.92	34	25	1.60	−0.22
8	Cu(II)	L^{5b}	cat	5	[51]	2.03	2.37	2.02	2.02	8.44	0.86	1.09	2.95	3.97	31	20	1.62	−0.25
9	Cu(II)	L^{5b}	cat	5	[51]	2.03	2.36	2.00	1.98	8.37	0.86	1.1	2.94	3.94	32	18	1.62	−0.25
10	Cu(II)	L^{1b}	NO_3	6	[b]	2.00	2.28	2.00	2.00	8.28	0.88	1.07	2.90	3.95	31	16	1.56	−0.21
11	Cu(II)	L^{2b}	Cl	5	[b]	2.03	2.36	2.00	2.01	8.40	0.86	1.09	2.94	3.94	30	22	1.62	−0.24
12	Cu(II)	L^{3b}	Cl	5	[48]	2.15	2.12	2.06	2.06	8.39	1.01	1.04	2.93	4.08	45	35	1.55	0.02
13	Cu(II)	L^{3b}	$NCCH_3$	5	[48]	2	2.38	2.05	2.08	8.51	0.84	1.06	2.93	4.03	28	21	1.61	−0.28
14	Fe(II)	L^{1a}	$(NCS)_2$	6	[52]	2.24	2.37	2.17	2.18	8.96	0.95	1.06	2.92	4.2	39	33	1.78	−0.10
15	Fe(II)	L^{1a}	$(OAC)_2$	6	[52]	2.27	2.45	2.18	2.18	9.08	0.93	1.08	2.91	4.21	37	25	1.86	−0.15
16	Fe(II)	L^{1a}	(piv)(trif)	6	[52]	2.27	2.36	2.19	2.19	9.01	0.96	1.06	2.93	4.21	38	26	1.79	−0.08
17	Fe(II)	L^{5b}	$(OH_2)_2$	6	[52]	2.19	2.34	2.16	2.18	8.87	0.94	1.04	2.92	4.22	36	22	1.73	−0.11
18	Fe(II)	L^{5b}	$(trif)(OH_2)$	6	[52]	2.20	2.36	2.17	2.17	8.90	0.93	1.05	2.94	4.22	37	29	1.74	−0.12
19	Mn(II)	L^{1a}	$(Cl)_2$	6	[56]	2.39	2.53	2.23	2.26	9.41	0.94	1.10	2.96	4.27	38	35	1.96	−0.12
20	Mn(II)	L^{1d}	$(Cl)_2$	6	[56]	2.35	2.44	2.23	2.23	9.25	0.96	1.07	2.98	4.27	42	37	1.87	−0.07
21	Mn(II)	L^{1c}	$(trif)_2$	6	[b]	2.30	2.35	2.21	2.23	9.09	0.98	1.05	2.96	4.27	39	31	1.79	−0.05
22	Mn(II)	L^{4b}	$(OAc)_2(OH_2)_2$	6	[b]	2.33	2.45	2.26	2.30	9.34	0.95	1.05	2.98	4.35	36	24	1.87	−0.10
23	Mn(II)	L^{4c}	(acac)	6	[b]	2.30	2.44	2.23	2.21	9.18	0.94	1.07	2.95	4.30	39	20	1.85	−0.11
24	Mn(II)	L^{4b}	$(ONO_2)_4$	(7)	[b]	2.31	2.41	2.29	2.31	9.32	0.96	1.03	2.98	4.38	42	46	1.83	−0.08
25	Mn(II)	L^{1a}	$(ONO_2)_2$	7	[b]	2.35	2.36	2.26	2.30	9.27	1.00	1.03	2.94	4.36	41	39	1.84	−0.01
26	Mn(II)	L^{1b}	$(OAC)OH_2$	7	[b]	2.37	2.39	2.28	2.30	9.34	1.00	1.04	2.94	4.32	34	21	1.87	−0.01
27	Cr(III)	L^{1c}	$(Cl)_2$	6	[b]	2.1	2.22	2.05	2.06	8.43	0.95	1.05	2.87	4.04	38	26	1.61	−0.09
28	Co(II)	L^{1b}	(ONO_2)	(6)	[45]	2.14	2.13	2.08	2.09	8.44	1	1.02	2.88	4.03	37	33	1.58	+0.02
29	Co(II)	L^{1b}	(OAc)	(6)	[b]	2.15	2.17	2.11	2.10	8.53	0.99	1.03	2.90	4.09	37	25	1.60	−0.01
30	Co(II)	L^{1b}	$(OH_2)_2$	6	[b]	2.16	2.22	2.09	2.12	8.59	0.97	1.04	2.92	4.1	36	26	1.63	−0.06
31	Co(II)	L^{1b}	$(OH_2)_2$	6	[b]	2.15	2.21	2.12	2.14	8.62	0.97	1.02	2.9	4.18	40	31	1.63	−0.06
32	Cu(I)	L^{1a}	$NCCH_3$	5	[6]	2.29	2.19	2.17	2.24	8.89	1.05	1.02	2.97	4.21	39	35	1.68	+0.08
33	Cu(I)	L^{1a}	$NCCH_3$	5	[6]	2.24	2.16	2.25	2.38	9.03	1.04	0.95	2.95	4.41	41	42	1.63	+0.06
34	Cu(I)	L^{5a}	$NCCH_3$	5	[50]	2.23	2.18	2.25	2.34	9	1.02	0.96	2.95	4.37	40	45	1.64	+0.04
35	Cu(I)	L^{5a}	$NCCH_3$	5	[50]	2.2	2.2	2.21	2.49	9.1	1	0.94	2.95	4.45	42	42	1.63	+0.00
36	Cu(I)	L^{2a}	$NCCH_3$	5	[b]	2.21	2.21	2.29	2.30	9.01	1.00	0.96	2.93	4.50	39	38	1.65	+0.00
37	Cu(I)	L^{2a}	$NCCH_3$	5	[b]	2.24	2.22	2.22	2.39	9.07	1.01	0.97	2.95	4.37	37	34	1.67	+0.02
38	Zn(II)	L^{1b}	Cl	5	[b]	2.21	2.11	2.10	2.11	8.53	1.05	1.03	2.94	4.02	33	25	1.58	+0.07
39	Zn(II)	L^{1b}	Cl	5	[b]	2.19	2.1	2.09	2.12	8.5	1.04	1.02	2.94	4.04	35	27	1.56	+0.07
40	Zn(II)	L^{1b}	NO_3	6	[b]	2.16	2.13	2.11	2.11	8.51	1.01	1.02	2.95	4.08	38	35	1.56	+0.02

[a] cat = catecholate, OAc = acetate, piv = pivalate, trif = triflate, acac = acetylacetonate. [b] This work.

0947-6539/02/0824-5754 $ 20.00+.50/0 *Chem. Eur. J.* **2002**, *8*, No. 24

apparent from Figure 2a), the out-of-plane angle of the N_{py}–M vectors with respect to the pyridine planes ($3^\circ < \gamma < 18^\circ$; not given in Table 1) and the angle between the two pyridine planes ($15^\circ < \tau < 46^\circ$). It is obvious that these latter parameters, related to the relatively weak torsion around C^2–C^9, are correlated with the dislocation of the metal center within the rigid bispidine cavity. Intuitive geometric measures for this dislocation are the horizontal and vertical translation, *h* and *v*, respectively, of the metal ion from the center of the line through N3 and N7 (Scheme 3). Large values for *h* are

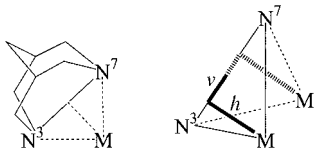

Scheme 3.

observed for large metal ions (large values for Σ(M–N)); positive values for *v* emerge for M–N3/M–N7 > 1, negative values for M–N3/M–N7 < 1 (this assumes that M lies on or very close to the plane through N3, N7, X, which has been shown to be the case). As expected from a geometric analysis, a plot of M–N3/M–N7 versus *v* is linear (see Supporting Information, Figure S1).

A plot of *v* versus *h* for all 40 structures is given in Figure 3. It emerges that, while the ligand is very rigid (Figure 2a), there is a high degree of elasticity in the coordination sphere.[47] The cluster with structures of copper(II) bispidine

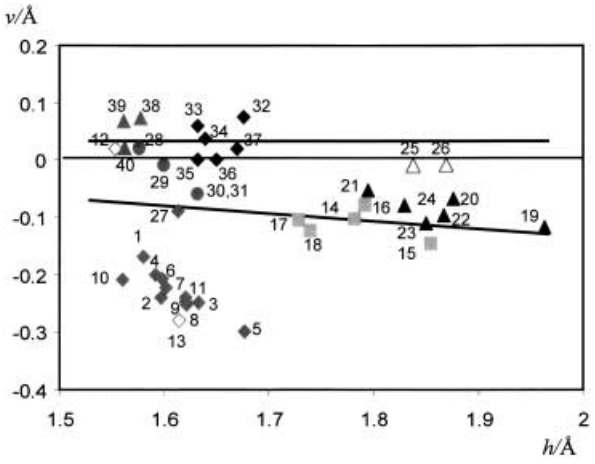

Figure 3. Plot of *v* versus *h* of all 40 stuctures from Table 1 (see Scheme 3 for the definition of *v* and *h*); the numbers correspond to those of Table 1, different symbols are used for different metal centers and/or ligands.

complexes (**1**–**11**) is well separated from all other datasets (at this point, the copper(II) structures **12** and **13** with L^3 (open diamonds) are not considered; also excluded from the following general discussion are structures **25**, **26**, open triangles, seven-coordinate manganese(II); see below). The separation of the copper(II) structures is probably caused by an electronically enhanced (Jahn–Teller lability of copper(II)) asymmetry of the optimal position of the metal ion in the rigid bispidine cavity. Indeed, inspection of the structures (see Figure 1, Figure 2) indicates that the tight five-membered chelate rings involving the pyridine donors enforce M–N3 < M–N4, and most structures with metal centers which generally do not lead to Jahn–Teller active states (e.g., chromium(III), manganese(II)) have $v < 0$. Therefore, it was unexpected that there are bispidine complexes with $v \geqslant 0$ (e.g., the copper(I) compounds **32**–**37**). Admittedly, the "cluster" of structures with $v \geqslant 0$ is, in terms of *v*, not well-separated from that with $v < 0$, that is, there might be a continuum rather than two distinct geomeric forms [the solid lines which suggest two separate clusters (and a third cluster with the copper(II) group of structures, see above) will be discussed below]. The fact that, apart from well-understood exceptions (see below), namely, cobalt(II) **28**, **29** versus **30**, **31** the copper(II) structures **12** versus **13**, and the two manganese structures **25**, **26**, groups of structures of a particular metal ion belong to one or the other structural type might justify the separation into two types of structures with $v < 0$ and one with $v \geqslant 0$.

An interesting observation is that, within a group of structures with a constant metal center (e.g., manganese(II)), there is a significant variation of metal–donor bond lengths, and this variation is generally much larger for the amine than for the pyridine donors (see Table 1). Part of this variation must result from the electronic influence exerted by the co-ligands; however, there must also be another reason since the two manganese(II) complexes **19** and **20** have identical donor sets. From pK_a determinations, photoelectron spectra, and molecular orbital calculations of diazaadamantane derivatives it emerges that keto groups in the "caps" (X = C=O in Scheme 1) lead to a reduction of the basicity of the amine donors as a result of through-bond interactions and inductive effects.[64] The data in Table 1 confirm this trend. Therefore, it is not unexpected that **19**, the only six-coordinate manganese(II) complex in this series with a keto group in the cap (X = C=O) has the longest Mn–N_{amine} bond lengths and therefore is moving out of the rigid bispidine cavity (large *h* and slightly decreasing *v*).

Of particular interest are the two structures of copper(II) coordinated to L^3 (**12** and **13**), with chloride and acetonitrile as co-ligands, respectively. While **13**, with a coordinated acetonitrile, has a typical copper(II) structure ($v = -0.28$) that with chloride (**12**) leads to an inversion of the Jahn–Teller axis (M–N3 is considerably longer than in all other copper(II) structures, M–N7 is much shorter than usual and M–N3 is a little but significantly longer than M–N7, leading to a positive *v* ($v = +0.02$); the metal–pyridine bond lengths are as usual; see Figure 3 and Table 1). The structure is still square pyramidal, with the co-ligand Cl^- in-plane (similar bond length as in **1**), but with N3 instead of N7 as the apical donor (see Figure 4). A DFT analysis reproduced this structural feature and indicated that the Cu–Cl bonding energy is significantly smaller than in structures with N7 as the axial donor and that this "isomer" is less stable;[46] the predicted complex stability and Cu–Cl bond energy differences are well supported experimentally by the corresponding reduction potentials[49, 50] and stability constants for chloride binding.[58] Our present analysis indicates that constraints of the ligand backbone lead to a situation where M–N3 may become longer than M–N7 but the M–N3/M–N7 ratio (average of 0.86 for

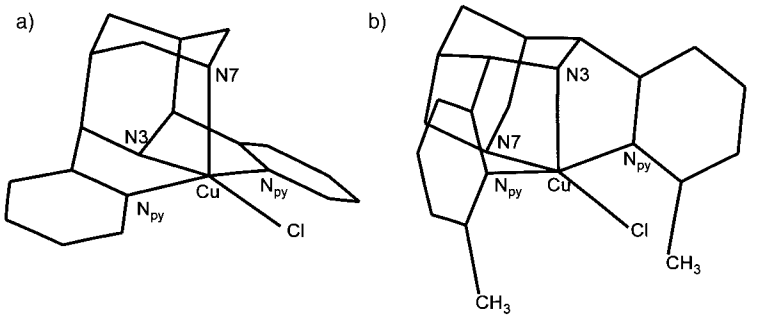

Figure 4. Plots of the experimental structures of a) $[Cu(L^1)(Cl)]^{+}$[6] (Cu–N3 = 2.04 Å, Cu–N7 = 2.30 Å) and b) $[Cu(L^3)(Cl)]^{+}$[48] (Cu–N3 = 2.15 Å, Cu–N7 = 2.12Å).

the $Cu^{II}(L^1)$-fragment versus 1.01 in **12**) may not be inverted. This leads to a quenching of the Jahn–Teller stabilization, and also emerges from the published DFT analysis[46] and reduction potentials.[49, 50]

Molecular mechanics was used to analyze the elasticity of the tetradentate bispidine-type ligands (MOMEC97 program[65] and force field;[66] new parameters are given in the Experimental Section). Some ad hoc changes to the force field were necessary to improve the agreement with the experimental structures (note that these "new parameters" were not fully optimized and the computational results are used here only for qualitative purposes). The changes include a torsional potential for the copper(II)–pyridine bond, an out-of-plane potential for the copper(II)–pyridine vector with respect to the pyridine plane (these were assumed to be of importance but never introduced in MOMEC before because of a lack of experimental data,[66] see, however, ref. [67]). Jahn–Teller distortions were modeled with the conventional technique, based on two different sets of parameters for in-plane and axial bonding.[68, 69] It is interesting that, with the original force field, all computed copper(II)–donor bonds were too short. There are at least two plausible reasons for this: 1) the harmonic potentials used are too weak and/or 2) the original force field has been tuned to copper(II) amine chromophores with planar CuN_4 geometries, and these are electronically different from the copper-bispidine chromophores.[46]

For the evaluation of the size, shape, and elasticity of the bispidine cavity the constrained sum of all four metal–donor bonds was varied between 7 Å and 9 Å (average M–N bond length between 1.75 Å and 2.3 Å).[70] Curves of energy versus cavity size were computed for the metal-free ligand (k_{M-L} = 0.0; metal-ion-independent shape, size, and elasticity), for cobalt(III), copper(II), chromium(III), cobalt(II), nickel(II), and zinc(II) complexes; those for the ligand and for cobalt(II) (both "isomers") are shown in Figure 5. From the metal-ion-independent curve it emerges that the optimum size of the metal ion is quite large ($M-N_{av} \approx 2.15$ Å), that is, in the region of the observed bond lengths of the iron(II), cobalt(II), and zinc(II) complexes (see Table 1 and Figure 5, which also shows averaged observed M–L bond lengths for the various metal ions). The curve is rather flat for metal ions larger than the optimum size (e.g. copper(I), manganese(II)): there is only little strain induced to the ligand by coordination to large metal ions. This is also true for small metal ions to some extent. This result is not unexpected since the metal ion is at the "periphery" of the partly open coordination site and, therefore, does not lead to much distortion of the ligand backbone when it is moved out of it (the only major strain included in this analysis is metal-donor-ligand-backbone angular strain; note that the fact that the corresponding potentials are harmonic is an oversimplification).[47]

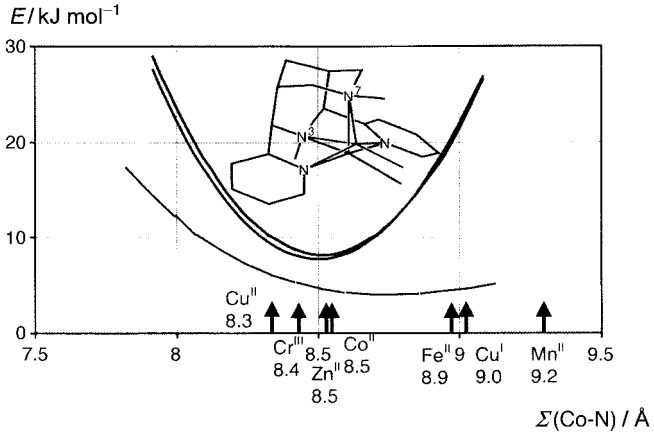

Figure 5. Cavity size and shape curves for the two "isomers" of $[Co(L^1)]^{2+}$; starting structures for the molecular mechanics calculations were structures **28** and **30**; it is unlikely but not excluded that there are other minimum structures ("isomers"); also included are averaged observed M–L bond lengths (arrows, for the data see Table 1).

The curves for the two possible "isomers" of cobalt(II) (and for the other metal ions not shown in Figure 5) are much steeper and reflect the strain induced by the ligand on the metal center; the minima reflect the preference of the metal ion for a specific metal–donor bond length. The two curves of the "isomers" of cobalt(II) (M–N3/M–N7 < 0, M–N3/M–N7 > 0) are nearly superimposable. However, the corresponding optimized minimum structures are significantly different (Co–N3, Co–N7, Co–N_{py}, h, v [Å]; 2.11, 2.19, 2.11, 1.6, −0.06; 2.16, 2.11, 2.19, 1.52, +0.037, respectively; the latter structure is similar to that described in the literature (entry 28 in Table 1 and Figure 3).[52] Similar differences are observed for all other pairs of structures with identical Σ(M–N) but lying on the two different curves. From this molecular mechanics analysis it follows that there are two distinct minima rather than a continuum of structures. From the two curves in Figure 5 it also emerges that the two structural forms are close to degenerate, an observation which is not unexpected in view of the shallow curve for the metal-free ligand (note that co-ligands and metal-centered electronic effects, excluded in this simple molecular mechanical analysis, might therefore be of importance for defining the position of the metal ion in the cavity). On the basis of these model calculations, it was expected that it might be possible to crystallize both geometric forms for cobalt(II). Figure 3 and Table 1 (structures

  0947-6539/02/0824-5756 $ 20.00+.50/0 *Chem. Eur. J.* **2002**, *8*, No. 24

28–**31**) indicate that two structures each (**28**, **29**/**30**, **31**; $v \sim 0$/$v < 0$) with different co-ligands may be attributed to the two clusters.

The geometric parameters h and v, which visualize the displacement of the metal ion from the center of the cavity of the cobalt(II)-bispidine fragment, derived from the molecular mechanical analysis, are plotted as solid lines in Figure 3. They underline the idea of two different clusters of structures (plus that of the Jahn–Teller distorted copper(II) structures). 1) The line defined by the computed curve for the cobalt(II) isomer with a short Co–N7 axis has $v = +0.04$ Å and passes through the Cu^{I}, Co^{II}[1], Zn^{II} cluster. 2) The line defined by the computed curve for the cobalt(II) isomer with a long Co–N7 axis indicates that v becomes slightly more negative with increasing metal ion size. This is in agreement with the observed structures of the Cr^{III}, Fe^{II}, Mn^{II}, Co^{II}[2] cluster. 3) The copper(II) complexes have a strongly negative value of v and a rather large dependence of v from subtle structural differences (sum of the bond lengths, Cu–N7/Cu–N3 ratio).

The molecular mechanics and geometric analyses, as well as the observed experimental structural data indicate that the two "isomeric" forms with long and short M–N7 axes are very close in energy and that the corresponding energy surface is very shallow. Therefore, metal ion preferences (amine versus pyridine donors), co-ligands, and solvation or crystal lattices are of importance for the stabilization of either structural type. It is interesting that there is a small but significant difference in the ratio of the metal–amine to metal–pyridine bond lengths between structures with a positive and negative parameter v (or M–N3/M–N7 ratio of 0.95 and 1.11, respectively, see Table 1). This indicates that relatively strong (and short) bonds to the pyridine donors prefer structures with negative v. Therefore, the copper(I) compounds with long $Cu–N^{py}$ bonds (see also[48]) are well accommodated in structures with long Cu–N3 bonds. Another possible interpretation of the observed copper(I) structures is that four-coordination allows for an increasing angle τ since there is no repulsion by axial ligands. Indeed, generally structures with a relatively short M–N7 bond are five-coordinate. This is so for the copper(I) structures, for the copper(II) structure **12** with L^3 and for the zinc(II) structures **38** and **39**; exceptions are the zinc(II) structure **40**, the cobalt(II) structures **28** and **29**, and the seven-coordinate manganese(II) structures **25** and **26**. The copper(II) structures **1**–**11**, **13** are five-coordinate and have a long M–N7 bond as a result of a Jahn–Teller distortion (see above).

Structures with a relatively short M–N7 and long M–N3 bond lengths which are not five-coordinate are the six-coordinate cobalt(II) structures **28** and **29** as well as the zinc(II) structure **40** with four-membered chelate rings involving NO_3^- or OAc^-. These compounds have a short equatorial bond to the co-ligand (≈2.07 Å), a long axial bond (≈2.3 Å) and a distorted N7-M-X axis (≈160°), that is, the interaction with the extra axial donor is weak. The other exceptions are the seven-coordinate manganese(II) compounds **25** and **26**, which have strong in-plane bonding (five donors) and relatively weak axial interactions. An interesting structure therefore is that of the manganese compound **24** which, in contrast to **25**, has the equatorial (bidentate) nitrate in a very asymmetric coordination geometry (2.22, 2.57 Å in **24** versus 2.28, 2.41 Å in **25**), that is, the former structure may be regarded as an intermediate between seven- and six-coordinate, and this supports the overall structural trends (see Figure 3 and Table 1). It follows that the co-ligands have a considerable influence in terms of the position of the metal ion inside the bispidine cavity.

A correlation between the type of donor X at the fifth and sixth coordination site, the corresponding M–X bond lengths and the M–N3/M–N7 ratio also emerges from the experimental structural parameters (not discussed here in detail, see caption to Figure 1)[50, 53] and preliminary DFT model calculations. These have been carried out for cobalt(II) complexes with one or two Cl^- or OH_2 as co-ligands and a slightly simplified bispidine backbone (CH_2 at C9, CH at C1, C5) or with a very simple model with four monodentate donors (NH_3 at N3, N7 and $HN{=}CH_2$ at the pyridine sites), in analogy to earlier DFT studies with the copper(II) complexes.[46] The preliminary results suggest that, in agreement with the force-field calculations, there is a very flat energy surface with two extreme structures with M–N3 ≥ M-N7 and M–N3 < M–N7. Also, in agreement with the experimental data, the bond lengths to the co-ligands are correlated with the distances to the amines in the *trans* position. An interesting feature is that the optimized structures and relative energies are strongly dependent on the number (one or two) and types of co-ligands.[71]

Conclusion

The metal–bispidine structures discussed here are clustered in two groups, with M–N3 = M–N7 and M–N3 < M–N7. The experimental structural data indicate that this differentiation is somewhat arbitrary. However, both molecular mechanical and DFT model calculations suggest that there are shallow energy minima on the energy surface. In terms of ligand strain, the two distinct clusters are close to degenerate. The electronic structure of the metal center and co-ligands are of importance for the stabilization of a particular geometric form, and this may lead to a significant change in stability and

Table 2. New force-field parameters (for published parameters see[66])

	bond stretch potentials		
Structural parameter	k_b[mdyn Å^{-1}]	r_0[Å]	
$Cu–N^{amine}_{in\text{-}plane}$	0.80	2.00	
$Cu–N^{amine}_{axial}$	0.30	2.15	
$Cu–N^{pyridine}$	0.80	1.97	
	Valence angle potentials		
structural parameter	k_θ[(mdyn Å rad^{-2}]	Θ_0[rad]	
$Cu\text{-}N^{pyridine}\text{-}C^{pyridine}$	0.05	2.094	
	Torsional potentials		
structural parameter	k_ϕ[mdyn Å]	m	ϕ_{offset}
$*Cu–N^{pyridine}*$	0.005	2.0	0.262
	Out-of-plane potentials		
structural parameter	k_{oop}[mdyn Å rad^{-2}]		
$C\text{-}N\text{-}C^{pyridine}\text{-}Cu$	2.00		

Table 3. Crystallographic data of **10**, $[Cu(L^{1b})(ONO_2)]NO_3 \cdot CH_3CN$; **11**, $[Cu(L^{2b})(Cl)]Cl \cdot CH_3OH$; **21**, $[Mn(L^{1c})(O_3SCF_3)_2]$; **22**, $[Mn_2(L^{4b})(O_2CCH_3)_2(OH_2)_2](O_2CCH_3)_2 \cdot 11H_2O$; **23**, $[Mn_2(L^{4c})(acac)_2](ClO_4)_2$; **24**, $[Mn_2(L^{4b})(ONO_2)_4] \cdot 1.5H_2O \cdot 6CH_3CN$; **25**, $[Mn(L^{1a})(ONO_2)_2] \cdot 2CH_3CN$; **26**, $[Mn(L^{1b})(O_2CCH_3)(OH_2)]PF_6 \cdot 2H_2O$; **27**, $[Cr(L^{1c})(Cl)_2]PF_6$; **29**, $[Co(L^{1b})(O_2CCH_3)]O_2CCH_3$; **30**, $[Co(L^{1b})(OH_2)_2](ClO_4)_2$; **31**, $[Co(L^{1b})(OH_2)_2]Cl_2 \cdot 2H_2O$; **36**, **37**, $[Cu(L^{2a})(NCCH_3)]BF_4$; **38**, **39**, $[ZN(L^{1b})(Cl)](ZnCl_4)_{0.5} \cdot CH_3CN$; **40**, $[Zn(L^{1b})(ONO_2)]NO_3 \cdot H_2O$

	10	**11**	**21**	**22**	**23**
formula	$C_{25}H_{31}CuN_7O_{12}$	$C_{25}H_{34}Cl_2CuN_4O_8$	$C_{26}H_{30}F_6MnN_4O_{12}S_2$	$C_{54}H_{92}Mn_2N_8O_{33}$	$C_{60}H_{70}Cl_2Mn_2N_8O_{26}$
M	685.11	653.00	823.60	1491.24	750.01
T[K]	103(2)	173(2)	173(2)	173(2)	173(2)
crystal system	triclinic	monoclinic	triclinic	monoclinic	monoclinic
space group	$P\bar{1}$	$P2_1/n$	$P\bar{1}$	$C2/c$	$P2_1/c$
a[Üo]	8.2798(5)	10.9520(2)	10.3834(2)	25.8439(4)	12.3541(6)
b[Å]	11.8390(7)	22.5705(4)	10.6443(2)	12.9398(2)	15.9731(8)
c[Å]	15.4431(9)	11.8450(2)	15.9704(3)	21.2132(3)	17.3008(9)
α[°]	79.1360(10)	90	77.3250(10)	90	90
β[°]	89.8490(10)	112.3240(10)	75.3990(10)	98.9220(10)	108.7080(10)
γ[°]	74.3640(10)	90	76.3110(10)	90	90
V[Å^3]	1429.80(15)	2708.54(8)	1635.45(5)	7008.17(18)	3233.6(3)
Z	2	4	2	4	2
ρ_{calcd}[g cm^{-3}]	1.591	1.601	1.672	1.413	1.541
μ[mm^{-1}]	0.841	1.061	0.633	0.454	0.565
F_{ooo}	710	1356	842	3144	1556
crystal size[mm]	0.32 × 0.27 × 0.25	0.25 × 0.36 × 0.45	0.24 × 0.10 × 0.10	0.40 × 0.40 × 0.37	0.43 × 0.35 × 0.15
Θ_{max}[°]	32.01	28.30	25.00	28.32	28.34
measured reflns	18468	23997	20387	46575	21953
unique reflns (R_{int})	9293 [0.0228]	6590 [0.029]	5760 [0.048]	8646 [0.044]	7776 [0.035]
parameters	540	483	470	622	573
GOF	1.037	1.077	1.070	1.028	0.987
$R1$	0.0310	0.0406	0.0552	0.0321	0.0405
$wR2$	0.0826	0.1094	0.1601	0.0903	0.1096
resid. electron density	0.606/ − 0.275	1.208/ − 1.617	0.990/ − 0.521	0.518/ − 0.209	0.566/ − 0.490

	24	**25**	**26**	**27**	**28**
formula	$C_{58}H_{71}Mn_2N_{18}O_{23.5}$	$C_{29}H_{35}MnN_8O_{11}$	$C_{25}H_{37}F_6MnN_4O_{11}P$	$C_{26.6}H_{35}Cl_2CrF_6N_{4.8}O_6P$	$C_{31}H_{36}CoN_4O_{11}$
M	752.85	726.59	769.50	785.86	699.57
T[K]	173(2)	173(2)	173(2)	173(2)	106(2)
crystal system	monoclinic	triclinic	triclinic	triclinic	monoclinic
space group	$P2_1/c$	$P\bar{1}$	$P\bar{1}$	$P\bar{1}$	$P2_1/c$
a[Üo]	11.8672(6)	10.5075(6)	10.1943(2)	20.3111(5)	10.644(4)
b[Å]	17.1373(9)	11.6223(7)	11.14730(10)	21.9601(5)	15.014(6)
c[Å]	16.5640(9)	13.6084(8)	14.6133(2)	22.3176(5)	20.615(8)
α[°]	90	96.963(4)	99.5610(10)	78.847(2)	90
β[°]	97.1700(10)	96.909(4)	91.6210(10)	86.311(2)	103.826(8)
γ[°]	90	99.078(4)	93.5710(10)	72.470(2)	90
V[Å^3]	3342.3(3)	1612.39(16)	1633.13(4)	9312.7(4)	3199(2)
Z	2	2	2	10	4
ρ_{calcd}[g cm^{-3}]	1.496	1.497	1.565	1.401	1.452
μ[mm^{-1}]	0.471	0.482	0.549	0.566	0.603
F_{ooo}	1565	756	794	4032	1460
crystal size[mm]	0.36 × 0.24 × 0.11	0.37 × 0.27 × 0.13	0.43 × 0.19 × 0.12	0.06 × 0.34 × 0.38	0.17 × 0.20 × 0.23
Θ_{max}[°]	28.30	28.38	28.29	23.26	32.05
measured reflns	23020	21700	22073	85264	42373
unique reflns (R_{int})	8085 [0.045]	7919 [0.057]	7958 [0.039]	26726 [0.072]	10987 [0.0376]
parameters	634	554	581	2195	553
GOF	0.954	1.047	1.031	1.041	1.048
$R1$	0.0493	0.0529	0.0348	0.0691	0.0467
$wR2$	0.1430	0.1564	0.0993	0.2280	0.1428
resid. electron density	1.251/ − 0.535	1.146/ − 0.596	1.088/ − 0.249	1.452/ − 0.800	1.916/ − 0.915

	30	**31**	**36**, **37**	**38**, **39**	**40**
formula	$C_{23}H_{32}Cl_2CoN_4O_{16}$	$C_{23}H_{36}Cl_2CoN_4O_{10}$	$C_{26}H_{31}BcuF_4N_5O_6$	$C_{25}H_{31}Cl_3N_5O_6Zn_{1.5}$	$C_{23}H_{30}N_6O_{13}Zn$
M	750.36	658.39	659.91	701.95	663.90
T[K]	106(2)	106(2)	173(2)	106(2)	106(2)
crystal system	monoclinic	orthorhombic	triclinic	monoclinic	triclinic
space group	$P2_1/c$	$P2_12_12_1$	$P\bar{1}$	Cc	$P\bar{1}$
a[Üo]	11.2690(15)	12.2931(15)	7.6468(10)	11.308(2)	10.727(2)
b[Å]	15.296(2)	13.0773(16)	18.872(5)	17.957(3)	11.259(2)
c[Å]	17.723(2)	17.534(2)	20.344(3)	29.383(5)	12.707(2)
α[°]	90	90	89.696(19)	90	70.962(4)
β[°]	106.789(3)	90	80.698(14)	99.903(4)	82.502(4)
γ[°]	90	90	82.022(19)	90	66.630(4)
V[Å^3]	2924.7(7)	2818.7(6)	2868.7(9)	5877.7(18)	1331.8(4)
Z	4	4	2	8	2
ρ_{calcd}[g cm^{-3}]	1.704	1.551	1.528	1.586	1.656
μ[mm^{-1}]	0.855	0.859	0.837	1.555	1.004
F_{ooo}	1548	1372	1360	2880	688
crystal size[mm]	0.28 × 0.18 × 0.13	0.27 × 0.20 × 0.09	0.24 × 0.23 × 0.20	0.28 × 0.15 × 0.15	0.27 × 0.17 × 0.15
Θ_{max}[°]	32.02	32.02	28.29	32.04	32.06
measured reflns	26931	29960	36174	103980	23137
unique reflns (R_{int})	9858 [0.0492]	9594 [0.0422]	36175 [0.0000]	19075 [0.0472]	9007 [0.0360]
parameters	564	505	808	924	500
GOF	1.015	1.034	1.045	1.049	1.031
$R1$	0.0457	0.0321	0.0732	0.0387	0.0409
$wR2$	0.1250	0.0757	0.2140	0.0881	0.1095
resid. electron density	0.749/ − 0.908	0.603/ − 0.360	1.079/ − 1.229	0.794/ − 0.484	0.858/ − 1.049

0947-6539/02/0824-5758 $ 20.00+.50/0 *Chem. Eur. J.* **2002**, *8*, No. 24

reactivity. The strong correlation of the M–N3/M–N7 ratio with the bonding to co-ligands (substrates) leads to important applications. With carefully modified bispidine ligands, such as with L^3 and with pentadentate ligands with an additional pyridine donor at N3 or N7, it is, therefore, possible to tune the catalytic activity, and this was demonstrated with the copper-catalyzed aziridination[50] and the iron-catalyzed epoxidation.[59]

Experimental Section

The ligands were prepared as reported in the literature,[48, 60, 72–74] the metal complexes were obtained by standard methods,[6, 48–53, 57, 60] and all were characterized by elemental analyses and spectroscopy. Single crystals for X-ray structure determinations were obtained by slow evaporation of the solvents or by solvent diffusion.

Force-field calculations were carried out with the MOMEC program[65] and force field;[66] cavity size curves were computed as described.[70] For the structure optimization of the copper(II) complexes some modifications of the force field were necessary (note that these new parameters were not fully refined and used here mainly for qualitative purposes, see Results and Discussion). The parameters not previously reported are given in Table 2.

DFT calculations were performed with Gaussian 98,[75] with the B3LYP functional and the 6–31+G(d) basis set for all atoms. No symmetry constraints were applied. $[Co(NH_3)_2(NHCH_2)_2(H_2O)_2]$ was used as a model in all calculations. All structures reported here are fully optimized.

Crystal structure determinations: Crystal data and experimental details are listed in Table 3. Intensity measurements were carried out on a Bruker-AXS Smart 1000 diffractometer with graphite-monochromated $Mo_{K\alpha}$ radiation ($\lambda = 0.71073$ Å) at low temperature.

Absorption corrections were performed (multiple scans of equivalent reflections, SADABS[76]). The structures were solved by direct methods and refined by full-matrix least-squares techniques based on F^2 of all data, with the SHELXTL programs.[77] All non-hydrogen atoms were refined anisotropically. Hydrogen atoms were localized in difference Fourier syntheses and refined isotropically (except in **21**, **27** and **36**, **37** and for some methyl groups or in disordered groups). In some structures disorder of anions, solvent molecules, or ester groups were observed. For **36** and **37** only twinned crystals were obtained. That structure was solved and refined with GEMINI[78] and SHELXL 97.

CCDC-187977 – CCDC-187991 contain the supplementary crystallographic data for this paper. These data can be obtained free of charge via www.ccdc.cam.ac.uk/conts/retrieving.html (or from the Cambridge Crystallographic Data Centre, 12 Union Road, Cambridge CB2 1EZ, UK; fax: (+44) 1223-336033; or deposit@ccdc.cam.uk).

Acknowledgement

Financial support by the German Science Foundation (DFG) is gratefully acknowledged.

[1] J. M. Harrowfield, S. B. Wild in *"Comprehensive Coordination Chemistry"*, *Vol. 1*, Pergamon Press, Oxford **1987**.
[2] A. G. Blackman, W. B. Tolman, *Structure and Bonding, Vol. 97*, Springer, Berlin **2000**, p. 179.
[3] R. R. Jacobson, Z. Tyeklar, A. Farooq, K. D. Karlin, S. Liu, J. Zubieta, *J. Am. Chem. Soc.* **1988**, *110*, 3690.
[4] Kitajima, *J. Am. Chem. Soc.* **1989**, *111*, 8975.
[5] J. A. Halfen, S. Mahapatra, E. C. Wilkinson, S. Kaderli, V. G. Young, L. Que, Jr., A. D. Zuberbühler, W. B. Tolman, *Sience* **1996**, *271*, 1397.
[6] H. Börzel, P. Comba, C. Katsichtis, W. Kiefer, A. Lienke, V. Nagel, H. Pritzkow, *Chem. Eur. J.* **1999**, *5*, 1716.
[7] L. Que, Jr., W. B. Tolman, *Angew. Chem.* **2002**, *114*, 1160; *Angew. Chem. Int. Ed.* **2002**, *41*, 1114.
[8] F. A. Cotton, R. A. Walton, *Multiple bonds between metal atoms*, Oxford University Press, Oxford, UK **1993**.
[9] J. E. McGrady, R. Stranger, T. Lovell, *J. Phys. Chem. A* **1997**, *101*, 6265.
[10] R. Stranger, J. E. McGrady, T. Lovell, *Inorg. Chem.* **1998**, *37*, 6795.
[11] L. F. Lindoy, I. M. Atkinson, *Self-Assembly in Supramolecular Systems in Monographs in Supramolecular Chemistry* (Ed.: J. F. Stoddard), RSC, Cambridge **2000**.
[12] D. J. Cardenas, A. Livoreil, J.-P. Sauvage, *J. Am. Chem. Soc.* **1996**, *118*, 11980.
[13] R. A. Bissell, E. Cordova, A. E. Kaifer, J. F. Stoddart, *Nature* **1994**, *369*, 133.
[14] L. Zelikovich, J. Libman, A. Shanzer, *Nature* **1995**, *374*, 790.
[15] C. Belle, J.-L. Pierre, E. Saint-Aman, *New. J. Chem.* **1998**, 1399.
[16] T. R. Ward, A. Lutz, S. P. Parel, J. Ensling, P. Gütlich, P. Buglyo, C. Orvig, *Inorg. Chem.* **1999**, *38*, 5007.
[17] W.-D. Stohrer, R. Hoffmann, *J. Am. Chem. Soc.* **1972**, *94*, 779.
[18] W.-D. Stohrer, R. Hoffmann, *J. Am. Chem. Soc.* **1972**, *94*, 1661.
[19] J. Chatt, L. Manojovic-Muir, K. W. Muir, *Dalton Trans.* **1972**, 686.
[20] K. Wieghardt, G. Backes-Dahmann, B. Nuber, J. Weiss, *Angew. Chem.* **1985**, *97*, 773; *Angew. Chem. Int. Ed. Engl.* **1985**, *24*, 777.
[21] Y. Jean, A. Lledos, J. K. Burdett, R. Hoffmann, *J. Am. Chem. Soc.* **1988**, *110*, 4506.
[22] G. Parkin, *Acc. Chem. Res.* **1992**, *25*, 455.
[23] G. Parkin, *Chem. Rev.* **1993**, *93*, 887.
[24] F. A. Cotton, G. Wilkinson, C. A. Murillo, M. Bochmann, *Advanced Inorganic Chemistry*, 6th ed., Wiley New York, Chichester, Weinheim, Brisbane, Singapore, Toronto **1999**.
[25] P. Gütlich, H. A. Goodwin, D. N. Hendrickson, *Angew. Chem.* **1994**, *106*, 441; *Angew. Chem. Int. Ed. Engl.* **1994**, *33*, 425.
[26] G. Parkin, R. Hoffmann, *Angew. Chem.* **1994**, *106*, 1530; *Angew. Chem. Int. Ed. Engl.* **1994**, *33*, 1462.
[27] U. Kölle, J. Kossakowski, N. Klaff, L. Wesemann, U. Englert, G. E. Herberich, *Angew. Chem.* **1991**, *103*, 732; *Angew. Chem. Int. Ed. Engl.* **1991**, *30*, 690.
[28] U. Kölle, H. Luekeu, K. Handrick, K. Schilder, J. K. Burdett, S. Balleza, *Inorg. Chem.* **1995**, *34*, 6273.
[29] J. E. McGrady, *Angew. Chem.* **2000**, *112*, 3216; *Angew. Chem. Int. Ed.* **2000**, *39*, 3077.
[30] K. Yoon, G. Parkin, A. L. Rheingold, *J. Am. Chem. Soc.* **1992**, *114*, 2210.
[31] K. Yoon, G. Parkin, A. L. Rheingold, *J. Am. Chem. Soc.* **1991**, *113*, 1437.
[32] P. J. Desrochers, K. W. Nebesny, M. J. Labarre, M. A. Bruck, G. F. Neilson, R. P. Sperline, J. H. Enemark, G. Backes, K. Wieghardt, *Inorg. Chem.* **1994**, *33*, 15.
[33] J. Song, M. B. Hall, *Inorg. Chem.* **1991**, *30*, 4433.
[34] F. A. Cotton, L. M. Daniels, G. T. Jordan IV, *Chem. Commun.* **1997**, 421.
[35] M. M. Rohmer, A. Strich, M. Bénard, J. P. Malrieu, *J. Am. Chem. Soc.* **2001**, *123*, 9126.
[36] R. Clérac, F. A. Cotton, L. M. Daniels, K. R. Dunbar, C. A. Murillo, X. Wang, *Inorg. Chem.* **2001**, *40*, 1256.
[37] V. M. Miskowski, S. Franzen, A. P. Shreve, M. R. Ondrias, S. E. Wallace-Williams, M. E. Barre, W. H. Woodruff, *Inorg. Chem.* **1999**, *38*, 2546.
[38] B. A. Jazdzewski, P. L. Holland, M. Pink, V. G. Young Jr., D. J. E. Spencer, W. B. Tolman, *Inorg. Chem.* **2001**, *40*, 6097.
[39] S. Franzen, V. M. Miskowski, A. P. Shreve, S. E. Wallace-Williams, W. H. Woodruff, M. R. Ondrias, M. E. Barr, L. Moore, S. G. Boxer, *Inorg. Chem.* **2001**, *40*, 6375.
[40] K. Pierloot, J. O. A. De Kerpel, U. Ryde, B. O. Roos, *J. Am. Chem. Soc.* **1997**, *119*, 218.
[41] K. Pierloot, J. O. A. DeKerpel, U. Ryde, M. H. M. Olsson, B. O. Roos, *J. Am. Chem. Soc.* **1998**, *120*, 13156.
[42] U. Ryde, M. H. M. Olsson, B. O. Roos, A. C. Borin, *Theor. Chem. Acc.* **2001**, *105*, 452.
[43] P. Comba, R. Remenyi, *J. Comput. Chem.* **2002**, *23*, 697.
[44] C. Buning, G. W. Canters, P. Comba, C. Dennison, L. Jeuken, M. Melter, J. Sanders-Loehr, *J. Am. Chem. Soc.* **2000**, *122*, 204.
[45] P. Comba, R. Remenyi, unpublished results.
[46] P. Comba, A. Lienke, *Inorg. Chem.* **2001**, *40*, 5206.
[47] P. Comba, W. Schiek, *Coord. Chem. Rev.*, in press.

  0947-6539/02/0824-5759 $ 20.00+.50/0

[48] H. Börzel, P. Comba, K. S. Hagen, C. Katsichtis, H. Pritzkow, *Chem. Eur. J.* **2000**, *6*, 914.
[49] H. Börzel, P. Comba, K. S. Hagen, M. Kerscher, H. Pritzkow, M. Schatz, S. Schindler, O. Walter, *Inorg. Chem.* **2002**, *41*, 5440.
[50] P. Comba, M. Merz, H. Pritzkow, unpublished results.
[51] H. Börzel, P. Comba, H. Pritzkow, *Chem. Commun.* **2001**, 97.
[52] P. Comba, B. Nuber, A. Ramlow, *J. Chem. Soc. Dalton Trans.* **1997**, 347.
[53] H. Börzel, P. Comba, K. S. Hagen, M. Merz, Y. D. Lampeka, A. Lienke, G. Linti, H. Pritzkow, L. V. Tsymbal, *Inorg. Chim. Acta* **2002**, *337*, 408.
[54] G. D. Hosken, R. D. Hancock, *J. Chem. Soc. Chem. Commun.* **1994**, 1363.
[55] G. D. Hosken, C. C. Allan, J. C. A. Boeyens, R. D. Hancock, *J. Chem. Soc. Dalton Trans.* **1995**, 3705.
[56] P. Comba, H. Pritzkow, W. Schiek, *Angew. Chem.* **2001**, *113*, 2556; *Angew. Chem. Int. Ed.* **2001**, *40*, 2465.
[57] H. Börzel, P. Comba, M. Kerscher, S. Kuwata, G. Laurenczy, G. A. Lawrance, A. Lienke, M. Merz, H. Pritzkow, unpublished results.
[58] P. Comba, M. Kerscher, A. Roodt, unpublished results.
[59] M. Bukowski, P. Comba, M. Merz, L. Que, Jr., unpublished results.
[60] P. Comba, B. Kanellakopulos, C. Katsichtis, A. Lienke, H. Pritzkow, F. Rominger, *J. Chem. Soc. Dalton Trans.* **1998**, 3997.
[61] C. K. Johnson, ORTEP, A Thermal Ellipsoid Plotting Program, Oak National Laboratories, Oak Ridge, TN 1965.
[62] S. P. Artz,D. J. Cram, *J. Am. Chem. Soc.* **1984**, *106*, 2160.
[63] D. J. Cram, G. M. Lein, T. Kaneda, R. C. Helgeson, C. B. Knobler, E. Maverick, K. N. Trueblood, *J. Am. Chem. Soc.* **1981**, *103*, 6228.
[64] R. Gleiter, M. Kobayashi, J. Kuthan, *Tetrahedron* **1976**, *32*, 2775.
[65] P. Comba, T. W. Hambley, N. Okon, G. Lauer, in *MOMEC97, a molecular modeling package for inorganic compounds*, Heidelberg **1997**.
[66] J. E. Bol, C. Buning, P. Comba, J. Reedijk, M. Ströhle, *J. Comput. Chem.* **1998**, *19*, 512.
[67] D. E. Reichert, M. J. Welch, *Coord. Chem. Rev.* **2001**, *212*, 111.
[68] P. Comba, *Coord. Chem. Rev.* **1993**, *123*, 1.
[69] P. Comba, M. Zimmer, *Inorg. Chem.* **1994**, *33*, 5368.
[70] P. Comba, N. Okon, R. Remenyi, *J. Comput. Chem.* **1999**, *20*, 781.
[71] P. Comba, R. Remenyi, unpublished results.
[72] R. Haller, *Arch. Pharm.* **1968**, *301*, 741.
[73] R. Haller, *Arch. Pharm.* **1969**, *302*, 113.
[74] U. Holzgrabe, E. Ericyas, *Arch. Pharm. (Weinheim, Germany)* **1992**, *325*, 657.
[75] M. J. Frisch, G. W. Trucks, H. B. Schlegel, G. E. Scuseria, M. A. Robb, J. R. Cheeseman, V. G. Zakrzewski, J. Montgomery, Jr., R. E. Stratmann, J. C. Burant, S. Dapprich, J. M. Millam, A. D. Daniels, K. N. Kudin, M. C. Strain, O. Farkas, J. Tomasi, V. Barone, M. Cossi, R. Cammi, B. Mennucci, C. Pomelli, C. Adamo, S. Clifford, J. Ochterski, G. A. Petersson, P. Y. Ayala, Q. Cui, K. Morokuma, D. K. Malick, A. D. Rabuck, K. Raghavachari, J. B. Foresman, J. Cioslowski, J. V. Ortiz, B. B. Stefanov, G. Liu, A. Liashenko, P. Piskorz, I. Komaromi, R. Gomperts, R. L. Martin, D. J. Fox, T. Keith, M. A. Al-Laham, C. Y. Peng, A. Nanayakkara, C. Gonzalez, M. Challacombe, P. M. W. Gill, B. Johnson, W. Chen, M. W. Wong, J. L. Andres, C. Gonzalez, M. Head-Gordon, E. S. Replogle, J. A. Pople, Gaussian 98, Gaussian, Inc., Pittsburgh PA, 1998.
[76] G. M. Sheldrick, Universität Göttingen, **2001**.
[77] G. M. Sheldrick, SHELXTL 5.1, Bruker-AXS, Madison, WI, **1998**.
[78] Bruker-AXS, Madison, WI, USA, **1999**.

Received: July 10, 2002 [F4232]

  0947-6539/02/0824-5760 $ 20.00+.50/0